CORA Cork Open Research Archive
Cartlann Taighde Oscailte Chorcaí

Title	Frequency adjustable MEMS vibration energy harvester
Authors	Podder, Pranay;Constantinou, Peter;Amann, Andreas;Roy, Saibal
Publication date	2016-11-01
Original Citation	Podder, P. Constantinou, P., Amann, A, and Roy, S. (2016) 'Frequency adjustable MEMS vibration energy harvester', Journal of Physics: Conference Series, 757, 012037 (6pp). doi: 10.1088/1742-6596/757/1/012037
Type of publication	Article (peer-reviewed)
Link to publisher's version	10.1088/1742-6596/757/1/012037
Rights	© 2016, The Authors. Published under licence in Journal of Physics: Conference Series by IOP Publishing Ltd. Content from this work may be used under the terms of the Creative Commons Attribution 3.0 licence. Any further distribution of this work must maintain attribution to the author(s) and the title of the work, journal citation and DOI. - https://creativecommons.org/licenses/by/4.0/
Download date	2026-10-27 06:15:48
Item downloaded from	https://hdl.handle.net/10468/3305

UCC
University College Cork, Ireland
Coláiste na hOllscoile Corcaigh

IOPscience iopscience.iop.org

Home Search Collections Journals About Contact us My IOPscience

Frequency adjustable MEMS vibration energy harvester

This content has been downloaded from IOPscience. Please scroll down to see the full text.

2016 J. Phys.: Conf. Ser. 757 012037

(http://iopscience.iop.org/1742-6596/757/1/012037)

View the table of contents for this issue, or go to the journal homepage for more

Download details:

IP Address: 143.239.102.113
This content was downloaded on 21/11/2016 at 10:10

Please note that terms and conditions apply.

You may also be interested in:

A low frequency MEMS energy harvester scavenging energy from magnetic field surrounding an AC current-carrying wire
Oskar Z. Olszewski, Ruth Houlihan, Alan Mathewson et al.

A non-linear 3D printed electromagnetic vibration energy harvester
P Constantinou and S Roy

Impulse-Excited Energy Harvester based on Potassium-Ion- Electret
H Ashizawa, H Mitsuya, K Ishibashi et al.

Design of an electromagnetic-transducer energy harvester
L Simeone, M Ghandchi Tehrani and S J Elliott

Energy harvester for use on nearby current-carrying conductors
Duy-Son Nguyen, Zhiwei Wu and Richard White

Self-sufficient electronic control for nonlinear, frequency tunable, piezoelectric vibration harvesters
S Heller, S Neiss, M Kroener et al.

Frequency adjustable MEMS vibration energy harvester

P Podder[1], P Constantinou[1], A Amann[2, 3] and S Roy[1, 4]

[1] Micro-Nano Systems Centre, Tyndall National Institute, Cork, Ireland
[2] Photonics Centre, Tyndall National Institute, Cork, Ireland
[3] School of Mathematical Sciences, University College Cork, Cork, Ireland
[4] A.S. Paintal Chair Professor in Engineering, Indian National Science Academy

Email: saibal.roy@tyndall.ie

Abstract. Ambient mechanical vibrations offer an attractive solution for powering the wireless sensor nodes of the emerging "Internet-of-Things". However, the wide-ranging variability of the ambient vibration frequencies pose a significant challenge to the efficient transduction of vibration into usable electrical energy. This work reports the development of a MEMS electromagnetic vibration energy harvester where the resonance frequency of the oscillator can be adjusted or tuned to adapt to the ambient vibrational frequency. Micro-fabricated silicon spring and double layer planar micro-coils along with sintered NdFeB micro-magnets are used to construct the electromagnetic transduction mechanism. Furthermore, another NdFeB magnet is adjustably assembled to induce variable magnetic interaction with the transducing magnet, leading to significant change in the spring stiffness and resonance frequency. Finite element analysis and numerical simulations exhibit substantial frequency tuning range (25% of natural resonance frequency) by appropriate adjustment of the repulsive magnetic interaction between the tuning and transducing magnet pair. This demonstrated method of frequency adjustment or tuning have potential applications in other MEMS vibration energy harvesters and micro-mechanical oscillators.

1. Introduction

Over the last couple of decades, the rapid advancements in the field of low-power integrated electronics have led to significant reduction in size and power consumption of electronic devices [1]. Subsequently, these advancements propelled the drive towards the development of the "Internet-of-Things (IoT)", a responsive network of billions of sustainable wireless sensor nodes (WSNs) that would facilitate seamless interaction between the physical and the digital world [2]. In order to ensure the sustainability and reliable operation of such enormous and expansive networks, the problem of long-term power supply to the WSNs must be addressed [3]. Conversion of the many forms of ambient energy (e.g. light, thermal gradient, wind flow, mechanical vibrations etc.) into usable electrical energy to power the WSNs offers a viable solution to this problem. The sheer abundance of ambient vibrations in the increasingly urbanized landscapes provides an untapped source of energy to power the WSNs [4].

Despite the wide availability, efficient conversion of ambient vibrations into electricity is a formidable challenge [5], primarily due to immense variability in the vibration spectrum (e.g. resonant, random, variable frequency, impulse etc.) and amplitude (e.g. very weak, perceptible, strong etc.). Many of the reported vibration energy harvesting devices (VEHs) rely on linear resonant

Content from this work may be used under the terms of the Creative Commons Attribution 3.0 licence. Any further distribution of this work must maintain attribution to the author(s) and the title of the work, journal citation and DOI.
Published under licence by IOP Publishing Ltd

oscillator systems that are designed to operate efficiently only within a very narrow frequency range near the resonance [6, 7]. In recent years, researchers attempted to widen the frequency range with nonlinear oscillator based energy harvesters and VEH frequency tuning [8, 9] to match that of the ambient vibrations. While the nonlinear oscillators have their advantages (e.g. broader bandwidth) and disadvantages (e.g. co-existing low and high energy branches) [10-13], the frequency adjustment or tuning by electrical (e.g. load variation, piezoelectric patch) [14, 15] and mechanical (e.g. magnetic force, mass variation etc.) [16, 17] methods offer a viable alternative. However, most of the reported frequency adjustment mechanisms are complicated and has been deployed only in macro or meso-scale devices.

In this work we develop a miniaturized frequency adjustable MEMS electromagnetic VEH where the spring stiffness can be controlled through manipulation of the repulsive magnetic interaction between a pair of tiny magnets. We have demonstrated through finite element analysis and numerical simulation that a frequency range of more than 25% of the initial resonance can be achieved. The silicon spring structure and copper planar micro-coils are micro-fabricated using standard MEMS processes, followed by assembly with an adjustable screw mechanism. The proposed mechanism of frequency adjustment can be exploited in other VEHs or micro-mechanical oscillators for post-fabrication frequency tuning.

2. Design of frequency adjustable MEMS electromagnetic vibration energy harvester

The architecture of the proposed frequency adjustable MEMS electromagnetic VEH comprising micro-fabricated silicon spring and double-layer planar coil and sintered NdFeB magnets is illustrated in figure 1. The spring structure consists of four folded-arm cantilever beams supporting a cubic NdFeB magnet attached to the central paddle. The four folded cantilevers are attached to the two diagonally opposite corners of the movable central paddle such that large amplitude out-of-plane oscillation of the suspended magnet is facilitated, while in-plane torsional movement around the vertical out-of-plane axis is eliminated (Figure 1(c)). The spiral planar double-layer copper coil is positioned underneath the suspended transducing magnet such that maximum flux linkage is established in the transducing magnet-coil assembly (Figure 1(b)). A second cubic NdFeB magnet is positioned above the transducing magnet such that they interact via repulsive magnetic force. The extent of the magnetic repulsion can be controlled by precise manipulation of the gap between the magnets through a screw-mechanism. By precise manipulation of the repulsive magnetic force, the potential energy profile and the spring stiffness can be controlled, leading to adjustability of the resonance frequency. The different design parameters for the micro-VEH are given in table 1.

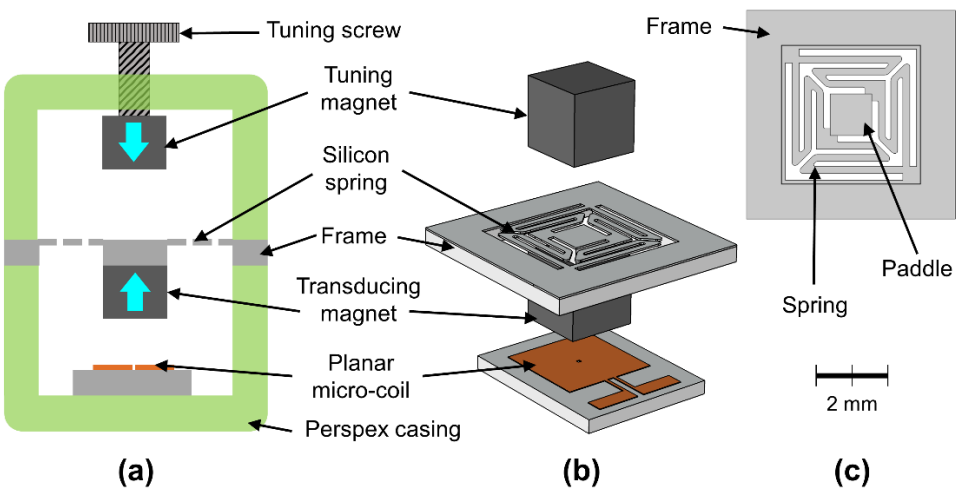

Figure 1. (a) Schematic diagram and (b) perspective view of the frequency adjustable micro-VEH. (c) The silicon spring structure with two diagonally clamped corners.

3. Finite element analysis on silicon spring and magnet-coil assembly

The vibrational modes and electromagnetic coupling factor are determined through finite element analysis using COMSOL Multiphysics and Ansoft Maxwell software tools. The first two modes (300.76 Hz and 318.9 Hz) are due to torsional motion of the combined paddle-magnet mass with axis along the diagonals in the spring plane (Figure 2(a)). The third mode (408.81 Hz) is the intended primary vibration mode, which represents a vertically oriented out-of-plane translational motion. The fourth mode (6291 Hz) is a complex combination of translational and torsional motions. Among all of these vibrational modes, the third mode produces the maximum relative displacement between the transducing magnet and coil. The distribution of magnetic flux densities in the device shows a substantial flux linkage between the vertically oriented transducing magnet and the planar coil (Figure 2(b)). Therefore, the vertically oriented motion (as in the third mode) of the transducing magnet will induce the optimal flux linkage gradient and generate maximum power.

Table 1. Micro-VEH device design parameters.

Parameter	Value
Silicon spring foot-print	6 mm × 6 mm
Spring thickness	50 µm
Spring arm width	200 µm
Planar micro-coil foot-print	4 mm × 5 mm
Number of coil turns	132 turns
Size of NdFeB magnets	2 mm × 2 mm × 2 mm

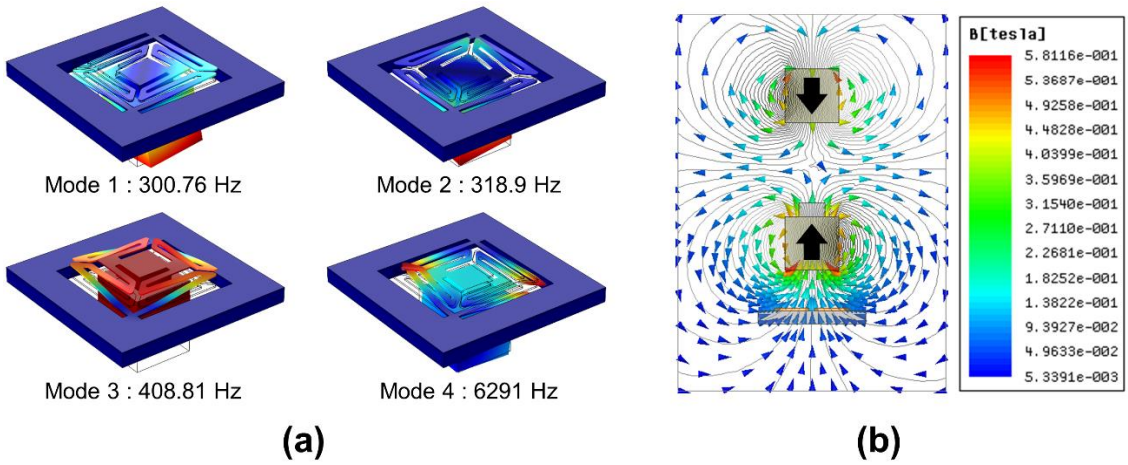

Figure 2. (a) The first four vibrational modes of the micro-VEH. Mode 3 shows the vertical translational motion, which is the intended vibration mode. (b) Magnetic flux distribution due to the tuning and transducing permanent magnets. Substantial flux linkage is established in the planar coil.

4. Numerical simulation results and discussion

A numerical model of the frequency adjustable micro-energy harvester is developed to study the effect of varying magnetic repulsion on the potential energy, spring stiffness and frequency response of the system. The total potential energy ($U(x)$) of the system, considering the spring stiffness (k) and the repulsive magnetic interaction between the transducing and tuning magnet can be expressed as [18],

$$U(x) = \frac{1}{2}kx^2 + \frac{\mu_0 p_1 p_2}{2\pi (d-x)^3} \tag{1}$$

where x is the vertical displacement of the transducing magnet, μ_0 is the air permeability, p_1 and p_2 are the magnetic dipole moments of the repulsively positioned transducing and tuning magnets respectively, and d is the vertical distance between the spring frame and the tuning magnet. The associated restoring force can be obtained by differentiating (1) as given below,

$$F(x) = -\frac{\partial}{\partial x}U(x) = -kx - \frac{3\mu_0 p_1 p_2}{2\pi(d-x)^4} \tag{2}$$

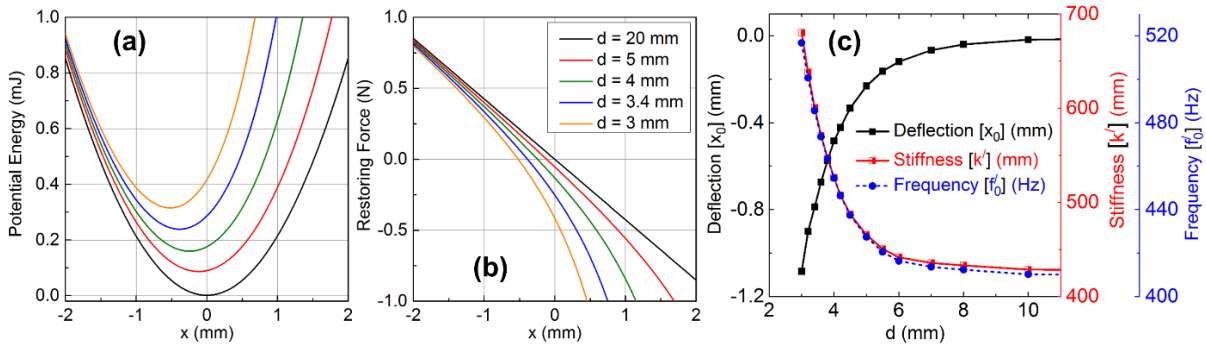

Figure 3. Variation of (a) potential energy profile and (b) restoring force with d. (c) With decreasing d, the spring deflects downward, and the stiffness and resonance frequency increases significantly.

The variation of the potential energy and restoring force profiles with d are illustrated in figure 3(a, b). With decreasing d, the potential energy profile become asymmetric, while the slope of restoring force become steeper, indicating increased linear spring stiffness which can be expressed as,

$$k^{/}(d) = \left[-\frac{\partial}{\partial x}F(x)\right]_{x=x_0} \tag{3}$$

where x_0 is the downward deflection of the movable paddle due to the repulsive force between the tuning and transducing magnets. The increasing spring stiffness with decreasing d results in increasing resonance frequency (Figure 3(c)). The complete dynamical system equation is given by,

$$m\ddot{x} + kx + \frac{3\mu_0 p_1 p_2}{2\pi(d-x)^4} + D\dot{x} + \gamma I = -m\ddot{y} \tag{4}$$

where m is the oscillating equivalent mass, D is the mechanical damping factor, γ is the electromagnetic coupling factor, I is the current induced in the coil and $y = Y_0 \cos \omega t$ represents the vibratory displacement of the system. The simulation parameters are given in table 2. The numerical frequency sweep responses obtained by fourth-order Runge-Kutta method in Matlab shows increasing output power with increasing vibrational accelerations (figure 4(a)). At 1g, the device generates 18.7 μW power across 135 ohm resistive load. With decreasing d, the shift in the resonance frequency towards higher values are revealed (figure 4(b)), which shows more than 25% increase from the initial resonance frequency. Therefore, the frequency adjustment effect by manipulation of the repulsive magnetic interaction is validated through numerical simulations.

Table 2. Micro-VEH device simulation parameters.

Parameter	Symbol	Value
Equivalent mass	m	6.45×10^{-5} kg
Spring stiffness	k	425.5 N m^{-1}
Permeability of air	μ_0	1.256×10^{-6} H m^{-1}
Magnetic moments	p_1, p_2	7.56×10^{-3} A m^2
Mechanical damping factor	D	2.27×10^{-4} kg s^{-1}
Electromagnetic coupling factor	γ	3.74×10^{-2} Wb m^{-1}

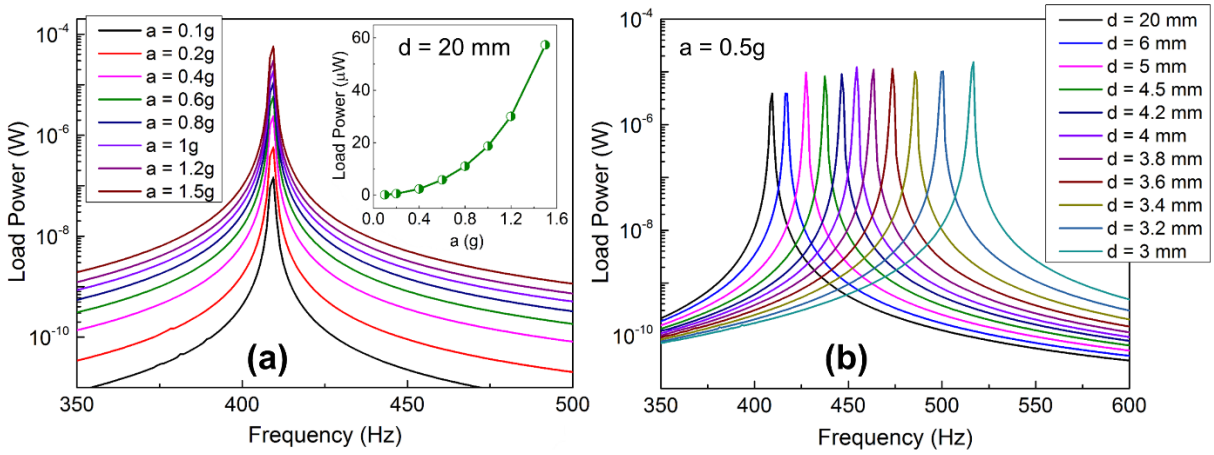

Figure 4. (a) Variation of load power with acceleration. At 0.4g and 1g, the micro-VEH produces 2.4 μW and 18.7 μW respectively. (b) Variation of the frequency response with decreasing *d*. The resonance frequency changes from 408.8 Hz to 516.2 Hz (> 25%) as *d* is varied from 20 mm to 3 mm

5. Fabrication of MEMS electromagnetic VEH

The principal components of the frequency adjustable MEMS electromagnetic vibration energy harvester are the silicon spring, the planar micro coil and the sintered NdFeB magnets. The silicon spring is fabricated on silicon-on-insulator (SOI) wafer with a 3 μm buried oxide layer in between the silicon device (50 μm) and handle (450 μm) layers. The spring patterns are first transferred onto the device layer by standard photolithography, followed by release of the springs via deep reactive ion etching (DRIE). The same process is applied on the backside (handle layer) to release the spring frame and the paddle and the individual springs (6mm × 6mm) are then diced off.

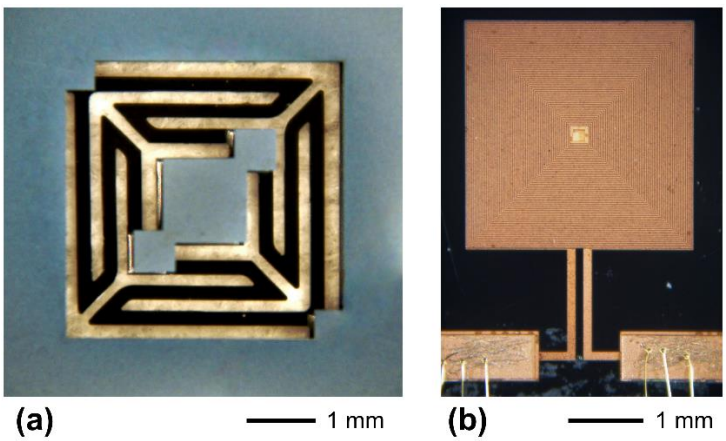

Figure 5. (a) The fabricated silicon spring structure, and (b) planar double-layer micro-coil

The planar double-layer micro-coils are fabricated using standard MEMS micro-fabrication processes, starting from silicon wafers with sputtered titanium-copper (20nm-200nm) seed layer. The first spiral coil layer pattern is then transferred photo-lithographically, and the copper coil layer is then electroplated (to a height of 15 μm) and seed layer is etched. Then, SU-8 photoresist layer is spin-coated on top of the first coil layer as insulation, and a central via is etched to connect to the second coil layer. A Ti-Cu seed layer is then sputtered on the insulating SU-8 layer, and the second coil layer is patterned and electroplated (12.5 μm). Finally, the seed layer is etched and the coil is spin-coated using SU-8 and connecting pads are opened, and the individual micro-coils are diced off.

The micro-fabricated silicon spring and double-layer planar coils (Figure 5(a, b)) are assembled together with the miniaturized NdFeB magnets and enclosed within a Perspex casing complete with the adjustable screw mechanism for stiffness and frequency adjustability.

6. Conclusion

We have shown the adjustability of the resonance frequency of an MEMS electromagnetic energy harvester through manipulation of magnetic repulsion force. This method of tuning the operational frequency of the micro-energy harvesters enable post-fabrication frequency adjustment for deployment in environments with different vibration frequencies. It has been demonstrated through finite element analysis and numerical simulations that precise manipulation of the repulsive magnetic interaction between the transducing and tuning magnet pair the spring stiffness and the resonance frequency can be adjusted to match any vibration frequency within a certain range (25% of initial resonance frequency). The frequency adjustable micro-generator prototype devices has been fabricated using standard MEMS micro-fabrication processes, which will be characterized to experimentally validate the results in the next phase. This frequency adjustment mechanism can potentially be deployed in other vibration energy harvesting devices and micro-mechanical oscillators.

Acknowledgements

This work is financially supported by Science Foundation Ireland (SFI) Principal Investigator (PI) project on 'Vibrational Energy Harvesting' grant no. SFI-11/PI/1201. The authors also would like to acknowledge the help provided by the Central Fabrication Facility (CFF) and their staff in Tyndall National Institute for silicon MEMS fabrication.

References

[1] T A C M Claasen, Proc. of the IEEE, Vol. 94, No. 6, June 2006.
[2] I F Akyildiz et al, Comput. Netw., vol. 51, pp. 921–960, 2007.
[3] H Sundmaeker et al., Cluster of European Research projects on the Internet of Things, 2010.
[4] S Roundy, J. Intell. Mater. Syst. Struct., vol. 16, pp. 809–823, Oct. 2005.
[5] S P Beeby et al, Meas. Sci. Technol. 17 (2006) R175–R195.
[6] P Glynne-Jones et al, Sens. Actuators A, vol. 110, pp. 344–349, 2004.
[7] S. P. Beeby et al, J. Micromech. Microeng., vol. 17, pp. 1257–1265, 2007.
[8] D Zhu et al, Meas. Sci. Technol. 21 (2010) 022001.
[9] L Tang et al, J. Int. Mat. Sys. Struct, Vol. 21, December 2010.
[10] A Erturk et al, Appl. Phys. Lett., vol. 94, art. no. 254102, (2009).
[11] B Marinkovic et al, Appl. Phys. Lett. 94, 103505 (2009).
[12] D Mallick, A Amann and S Roy, Smart Mater. Struct. 24 (2015) 015013.
[13] P Podder, D Mallick and S Roy, IoP Journal of Physics: Conference Series, 2014.
[14] V R Challa et al, Smart Mater. Struct. 17 (2008) 015035.
[15] D Mallick et al, Sens. Actuators A, 226, 154-162 (2015).
[16] D Guyomar et al, IEEE/ASME Trans. Mechatronics, Vol. 13, No. 5, October 2008.
[17] D Zhu et al, Sens. and Act. A: Physical Vol. 158, Issue 2, March 2010.
[18] P Podder et al, IEEE/ASME Transactions On Mechatronics, Vol. 21, NO. 2, April 2016.